Electronic Supplementary Information

Non-fullerene Acceptors with Alkylthiothiophene Side Chains for Efficient Non-halogenated Solvent Processed Indoor Organic Photovoltaics

Na Gyeong An,[a,‡] Ji Eun Lee, [b,‡] Woojin Lee,[a] Dohun Yuk,[a] Seyeong Song,[a] Chanjie Wang,[c] Soon-Ki Kwon,[c] Yun-Hi Kim,[b,*] and Jin Young Kim[a,*]

[a] Graduate School of Carbon Neutrality, School of Energy and Chemical Engineering, Ulsan National Institute of Science and Technology (UNIST), Ulsan 44919, South Korea.

[b] Department of Chemistry and RIGET, Gyeongsang National University, Jinju 52828, South Korea

[c] Department of Materials Engineering and Convergence Technology and ERI, Gyeongsang National University, Jinju 52828, South Korea.

[‡] These authors contributed equally.

*E-mail: jykim@unist.ac.kr; yhkim@gnu.ac.kr

Experimental Section

Material and Synthesis

PM6 (PBDB-T-2F, poly[(2,6-(4,8-bis(5-(2-ethylhexyl-3-fluoro)thiophen-2-yl)-benzo[1,2-b:4,5-b']dithiophene))-alt-(5,5-(1',3'-di-2-thienyl-5',7'-bis(2-ethylhexyl)benzo[1',2'-c:4',5'-c']dithiophene-4,8-dione)]) were purchased from solarmer. In case of ITIC-Th-s and ITIC-Th-s me acceptors, 2,-dithieno[3,2-b]thien-2-yl-1,4-benzenedicarboxylic acid-1,4-diethyl ester was prepared following the procedure described in the experimental section according to a known procedure reference.[1] All starting materials were purchased from Sigma Aldrich and Tokyo Chemical Industry.

Synthesis of 2,5-Dithieno[3,2-b]thien-2-yl-1,4- benzenedicarboxylic acid-1,4-diethyl ester (1)

The reaction was followed by the literature method. To a stirred solution of thieno[3,2-b]thiophene (421 mg, 3.0 mmol) in dry THF (10 mL) was added dropwise to a 2.5 M solution of n-butyllithium in hexane (1.2 mL, 3.0 mmol) at –78°C under nitrogen atmosphere. After being stirred for 30 min at –78°C, the resulting solution was warmed to –35°C and stirred for another 15 min. Then anhydrous zinc chloride (409 mg, 3.0 mmol) in dry THF (10 mL) was added to the mixture. The mixture was stirred for 1 h at 0°C and then the cooling bath was removed. Diethyl 2,5-dibromoterephthalate (456 mg, 1.2 mmol) and Pd(PPh₃)₄ (69 mg, 0.06 mmol) were added directly. The reaction mixture was refluxed overnight. Upon completion, the reaction mixture was filtered over celite, extracted with ethyl acetate and then dried over anhydrous MgSO₄. The product was purified by recrystallization (only dichloromethane) to afford a light yellow solid (400 mg, 67%). ^{1}H NMR (300 MHz, CDCl₃, ppm): 7.89 (s, 2H), 7.40 (d, 2H), 7.28 (d, 2H), 4.24 (m, 4H), 1.13 (t, 6H).
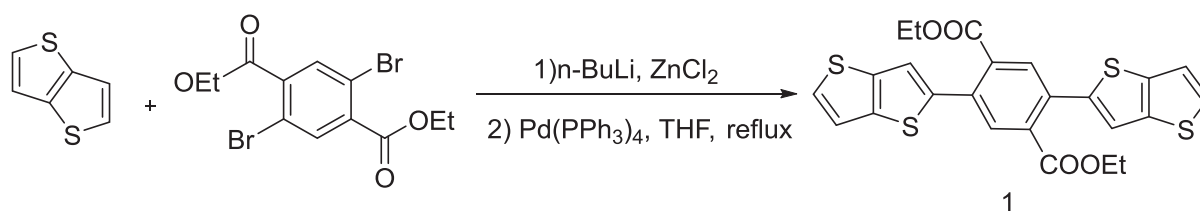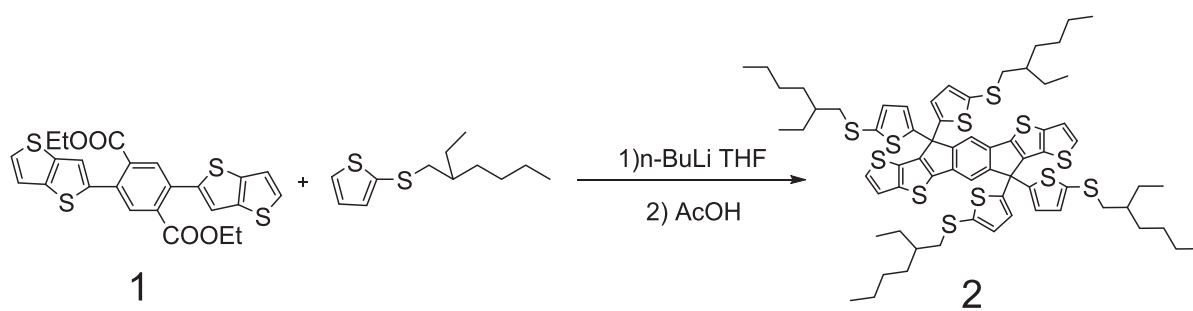

Scheme S1. Synthesis procedure of compound 1.

Synthesis of ITIC-Th-s (2)

To a solution of 2-(2-ethylhexylthio)thiophene (5.5 g, 24.0 mmol) in anhydrous THF (40 mL) at 0°C n-BuLi (9.6 mL, 24.0 mmol, 2.5 M in hexane) was added under nitrogen atmosphere. The mixture was stirred at 0°C for 1 h and then compound 1 (2.0 g, 4.0 mmol) in anhydrous

THF (40ml) was transferred to the mixture under N_2 at 0°C and stirred overnight. After quenching with water, the mixture was extracted with ethyl acetate. The combined organic phase was dried over $MgSO_4$. After evaporation of the solvent under reduced pressure, the crude product was purified by column chromatography on silica gel. The residue was dissolved in acetic acid (300ml) and then was stirred under reflux overnight. After cooling down to RT, the reaction mixture was poured into water and extracted with dichloromethane and then dried over anhydrous $MgSO_4$. The residue was purified by column chromatography on silica gel to afford ITIC-Th-s. (1.9 g, 37%). ^{1}H NMR (300 MHz, CD_2Cl_2, ppm): 7.60 (s, 2H), 7.32-7.24 (m, 4H), 6.82-6.77 (m, 8H), 2.69-2.67 (m, 8H), 1.40-1.32 (m, 8H), 1.30-1.10 (m, 28H), 0.79-0.69 (m, 24H); ^{13}C NMR (500 MHz, CD_2Cl_2, ppm): δ= 152.81, 147.54, 147.52, 144.71, 143.44, 142.46, 136.07, 135.24, 133.07, 132.06, 127.53, 126.74, 126.73, 120.40, 116.79, 57.13, 43.34, 39.08, 39.07, 31.96, 28.65, 25.22, 22.87, 13.85, 10.50. HRMS (FAB+): m/z calcd for ($C_{68}H_{82}S_{12}$) 1282.307; found 1282.47.

Scheme S2. Synthesis procedure of compound 2.
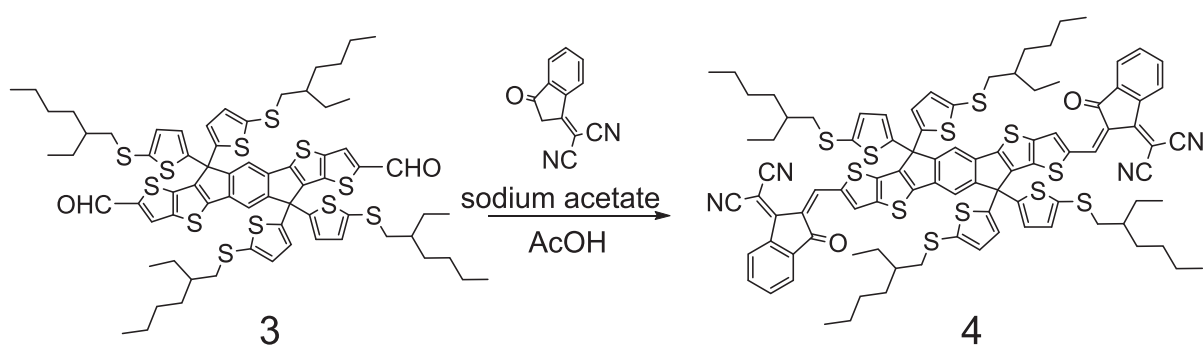
Synthesis of ITIC-Th-s-CHO (3)

To a solution of IT-thio-S-eth (1.9 g, 1.48 mmol) and DMF (2.16 g, 29.5 mmol) in anhydrous dichloroethane (65.2 mL) was added $POCl_3$ (2.27 g, 14.8 mmol) at 0°C under nitrogen atmosphere. The mixture was stirred under reflux overnight. After quenching with the solution of sodium acetate (1M) in the water, the mixture was extracted twice with ethyl acetate. The combined organic phase was dried over $MgSO_4$. After evaporation of the solvent under reduced pressure, the residue was purified by column chromatography on silica gel using hexane /dichloromethane (v/v = 1:2) as an eluent to afford ITIC-Th-s-CHO as a yellow solid (420 mg, 36%). ^{1}H NMR (300 MHz, $CDCl_3$, ppm): 9.97 (s, 2H), 8.01 (s, 2H), 7.77 (s, 2H), 6.93-6.87 (m, 8H), 2.81-2.79 (m, 8H), 1.53-1.45 (m, 8H), 1.44-1.20 (m, 28H), 0.88-0.80 (m, 24H); 13C NMR (500 MHz, CD2Cl2, ppm): δ= 182.80, 153.98, 149.38, 146.22, 145.29, 145.22, 142.41, 139.00, 136.71, 135.60, 132.09, 129.78, 127.04, 117.93, 57.21, 43.31, 39.10, 31.95, 28.63, 25.24, 22.85, 13.85, 10.52. HRMS (FAB+): m/z calcd for ($C_{70}H_{82}O_2S_{12}$) 1338.296; found 1338.357.
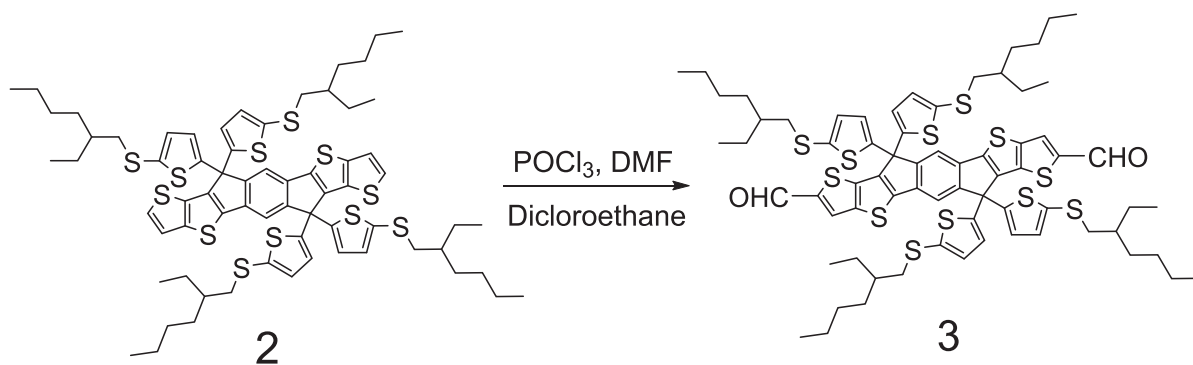
Scheme S3. Synthesis procedure of compound 3.

Synthesis of ITIC-Th-s (4)

1,1-dicyanomethylene-3-indanone (218.46 mg, 1.125 mmol) was added to a solution of sodium acetate(123.05 mg, 1.5 mmol) in the glacial acetic acid (15 mL) at 80°C under nitrogen atmosphere and then the mixture was stirred for 10 minutes. Then ITIC-Th-s-CHO (335 mg, 0.25 mmol) and toluene (15 mL) were added to the flask and the mixture was refluxed at 110°C overnight. Then the mixture was poured into water and extracted with dichloromethane. After evaporation of the solvent under reduced pressure, the residue was purified by recrystallization (dichloromethane/acetone) to afford a dark blue solid (220 mg, 52%). ^{1}H NMR (300 MHz, CD$_2$Cl$_2$, ppm): 8.94 (s, 2H), 8.75-8.72 (m, 2H), 8.27 (s, 2H), 7.98-7.81 (m, 8H), 7.02-6.99 (m, 8H), 2.85-2.83 (m, 8H), 1.57-1.44 (m, 8H), 1.43-1.21 (m, 28H), 0.85-0.80 (m, 24H); ^{13}C NMR (500 MHz, CD$_2$Cl$_2$, ppm): δ= 187.94, 160.20, 154.75, 152.05, 145.95, 145.47, 143.73, 140.07, 140.03, 137.80, 136.93, 136.39, 135.94, 135.31, 134.64, 132.06, 127.15, 125.27, 123.78, 123.71, 118.29, 114.57, 114.48, 70.14, 57.19, 43.34, 39.08, 31.93, 28.60, 28.57, 25.21, 22.85, 13.81, 10.49, 10.46. HRMS (FAB+): m/z calcd for (C$_{94}$H$_{90}$N$_4$O$_2$S$_{12}$) 1690.371; found 1690.3738.

Scheme S4. Synthesis procedure of compound 4 (ITIC-Th-s).

Synthesis of ITIC-Th-s-me (5)

ITIC-Th-s-me was synthesized by using a similar method as ITIC-Th-s. 2-(2,3-Dihydro-5&6-methyl-3-oxo-1H-inden-1-ylidene)propanedinitrile (234.2 mg, 1.125 mmol) was added to a solution of sodium acetate (123.05 mg, 1.5 mmol) in the glacial acetic acid (15 mL) at 80°C under nitrogen atmosphere and then the mixture was stirred for 10 minutes. Then IT-thio-S-eth-CHO (335 mg, 0.25 mmol) and toluene (15 mL) were added to the flask and the mixture was refluxed at 110°C overnight. Then the mixture was poured into water and extracted with dichloromethane. After evaporation of the solvent under reduced pressure, the residue was purified by recrystallization (dichloromethane/acetone) to afford a dark blue solid (230 mg, 53%). ^{1}H NMR (300 MHz, CD_2Cl_2, ppm): 8.89 (s, 2H), 8.62-8.52 (m, 2H), 8.26-8.24 (d, 2H), 7.88 (s, 2H), 7.87-7.61 (m, 4H), 7.01-6.98 (m, 8H), 2.84-2.82 (m, 8H), 2.60-2.58 (d, 6H), 1.55-1.47 (m, 8H), 1.44-1.20 (m, 28H), 0.84-0.80 (m, 24H); ^{13}C NMR (500 MHz, CD_2Cl_2, ppm): δ= 188.05, 160.23, 154.69, 151.75, 146.71, 146.01, 145.91, 145.15, 143.64, 139.99, 137.73, 137.37, 137.27, 136.88, 136.25, 136.06, 135.91, 132.07, 127.14, 125.16, 124.23, 124.04, 118.23, 114.74, 114.59, 69.24, 57.19, 43.34, 39.08, 31.93, 28.61, 28.57, 25.21, 22.85, 21.82, 13.82, 10.50, 10.46. HRMS (FAB+): m/z calcd for ($C_{96}H_{94}N_4O_2S_{12}$) 1718.403; found 1719.494.
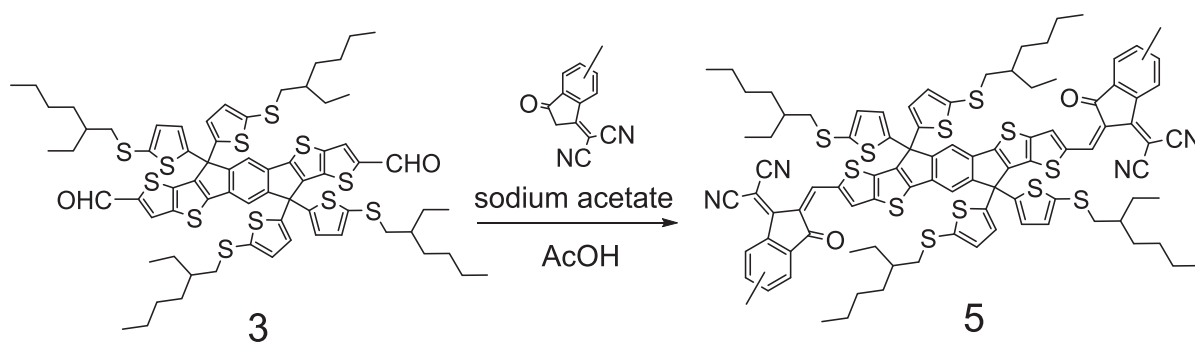
Scheme S5. Synthesis procedure of compound 5 (ITIC-Th-s-me).

Preparation of ZnO solutions

ZnO NP solutions were prepared using a method reported elsewhere, with a slight modification as follows. Zinc acetate dihydrate (2.95 g, 13.4 mmol) was dissolved in 135 mL of methanol at 60 °C. A KOH solution (1.48 g, 26.7 mmol of KOH in 55 mL methanol) was added dropwise to the zinc acetate solution under vigorous stirring and kept at 60 °C for 2 hours and 15 minutes. As-synthesized ZnO NPs were purified by precipitation and centrifugation twice using methanol. The precipitates were finally dispersed in methanol at a high concentration to make a stock solution (20–50 mg ml^{-1}). Before using it, the stock solution was diluted to the desired concentration (5–20 mg ml^{-1}).

ZnO sol-gel solutions were prepared by mixing diethylzinc (15 wt%) dissolved in toluene (Sigma Aldrich) and tetrahydrofuran (anhydrous, Sigma Aldrich) with a volumetric ratio as 1:2.

Measurements

^{1}H NMR and ^{13}C NMR spectra were recorded with an Advance 300 and DRX 500 MHz FT-NMR Bruker spectrometers, and chemical shifts (ppm) were reported with tetramethylsilane (TMS) as an internal standard. UV-vis absorption measurement for both solution and film states are conducted using 5000 UV-Vis-NIR spectrometer at room temperature. Film thicknesses were measured using a surface profiler (P6, KLA Tencor, USA). Cyclic voltammetry (CV) was recorded under a nitrogen atmosphere in a solution of Bu$_4$NClO$_4$ (0.1 M) in chloroform at a scan rate of 50 mVs^{-1}. A Pt wire was used as the counter electrode, and an Ag/AgNO$_3$ electrode was used as a reference electrode. The Ag/AgNO$_3$ electrode was calibrated using a Fc/Fc$^+$ redox couple as an internal standard, whose oxidation potential is set at −4.8 eV with respect to zero vacuum level. HOMO and LUMO energy levels were determined according to the equations ($E_{HOMO} = -(E_{ox}^{onset} - E_{Fc}^{onset} + 4.8)$ (eV)) and ($E_{LUMO} = -(E_{red}^{onset} - E_{Fc}^{onset} + 4.8)$ (eV)).

AFM height and phase images (5 μm × 5 μm) were obtained using a Multimode V microscope (Veeco, USA) in tapping mode. A dimension microscope running with a Nanoscope V controller was used to obtain AFM images of organic thin films. The images were measured in high-resolution tapping mode under ambient conditions. Silicon cantilevers (Bruker) with a resonant frequency of 300 kHz were used with a rotated tip to provide a more symmetric representation of features over 200 nm.

GIWAXS measurements were conducted at the PLS-II C&S UNIST-PAL(SAXS) (6D) beam line of Pohang Accelerator Laboratory. X-ray light coming from the in-vacuum undulator (IVU) was monochromated (E_k = 11.08 keV) using a Si (111) double crystal monochromator and focused horizontally and vertically at the sample position (450 (H) × 60 (V) μm^2 in FWHM) using a K–B-type focusing mirror system. The GIWAXS sample stage was equipped with a 7-axis motorized stage for the fine alignment of the sample and the incidence angle of X-rays was adjusted to 0.12°. GIWAXS patterns were recorded by a 2D CCD detector (SX165, Rayonix, USA), and X-ray irradiation time was 80–120s depending on the saturation level of the detector. Samples for GIWAXS measurements were prepared by spin-coating neat and blend solutions of the materials on top of silicon wafers.

Device Fabrication

ITO-coated glass substrates were firstly cleaned using a detergent, then ultrasonicated in acetone and isopropyl alcohol, followed by drying overnight in an oven. A PEDOT:PSS (Poly(3,4-ethylenedioxythiophene) polystyrene sulfonate, Baytron P VPAI 4083, H. C. Starck) aqueous solution was spin-cast and the substrates were baked for 10 min at 140 °C in air. Subsequently, the samples were transferred into a glove box to deposit the photoactive layer. Halogenated and non-halogenated solvent based active layer solution are formulated as following combinations; PM6:Acceptors (ITIC-Th-s and ITIC-Th-s-me) (D:A = 1:1, w/w) in chlorobenzene (CB): 1,8-diiodooctane (DIO) (99.5:0.5, v/v) (8 mg ml^{-1}) and PM6:Acceptors (D:A = 1:1, w/w) in o-xylene (Xyl): 1, 8-octanedithiol (ODT) (99.5:0.5, v/v) (7 mg ml^{-1}). All concentrations are indicated relative to the donor material. After the films were thermally

treated at 100 ºC for 10 min then dried in vacuum for 5 min, ZnO NPs layers were spin-cast. Devices were then completed by thermal evaporation of Al (100 nm) electrodes under a vacuum of approximately 2×10⁻⁶ Torr, yielding device active areas of 4 mm². For space charge limited current (SCLC) measurements, hole-only (glass/ITO/PEDOT:PSS/PM6:ITIC-Th-s or ITIC-Th-s-me/Au) and electron-only (glass/FTO/ZnO sol-gel/PM6:Acceptor/ZnO NPs/Al, FTO: fluorine-doped tin oxide) devices were fabricated, respectively. ZnO sol-gel layer was deposited at spin-rate of 3000 rpm then baked for 10 min at 110ºC in air.

Device Characterization

The current density–voltage (*J–V*) characteristics of the devices were measured using a Keithley 2365A source measurement unit. Under AM 1.5G condition, the device performance was estimated with an irradiation intensity of 100 W m⁻² which was calibrated with a standard silicon photodiode (PV Measurements, Inc.). EQE spectra were measured using a QEX7 quantum efficiency measurement system (PV Measurements, Inc.). Under indoor condition, the photovoltaic performance was estimated with an intensity adjustable a white LED in dark room at room temperature. All the devices were measured with a black colored shadow mask of 2.9 mm². The emission power spectrum of the LED light source at various light intensities was obtained by a calibrated fibre optics spectrometer (USB 4000, Ocean Optics, Inc., USA). With a combination of the emission power and EQE spectrum, the photon flux and integrated current density under the LED light source can be calculated from following equations.

$$J_{SC} = q \int EQE(\lambda)\Phi(\lambda)d\lambda \ \ [\mu A \ cm^{-2}]$$

$$H(\lambda) = qE\Phi(\lambda) = 10^{-6} * \frac{qhc}{\lambda}\Phi(\lambda) \ [\mu A \ cm^{-2} \ nm^{-1}]$$

where H (λ) and $\Phi(\lambda)$ are power spectrum and photon flux of the LED light source, h is planck constant (m² kg s⁻¹), c is speed of light (m s⁻¹), *q* is elementary charge (μA s) and λ is wavelength (m), respectively.

The charge mobilities were calculated by fitting the *J−V* characteristics of the single carrier diodes according to the Mott-Gurney relationship.

$$J_{SCLC} = \frac{9}{8}\frac{\varepsilon_r\varepsilon_0\mu V_a^2}{L^3}$$

Trap density (n_t) is calculated by following equation.[2]

$$n_t = \frac{2\varepsilon_r\varepsilon_0}{qL^2}V_{TFL}$$

It is noted that ε_r is the dielectric constant of the material, ε_o is the vacuum permittivity, μ is hole or electron mobility, L is the distance between the cathode which is equal to the film

thickness, V_a is the applied voltage and V_{TFL} is trap-filling limited voltage. Film thickness was measured using a profilometer (ST4000-DLX, KMAC, Korea).
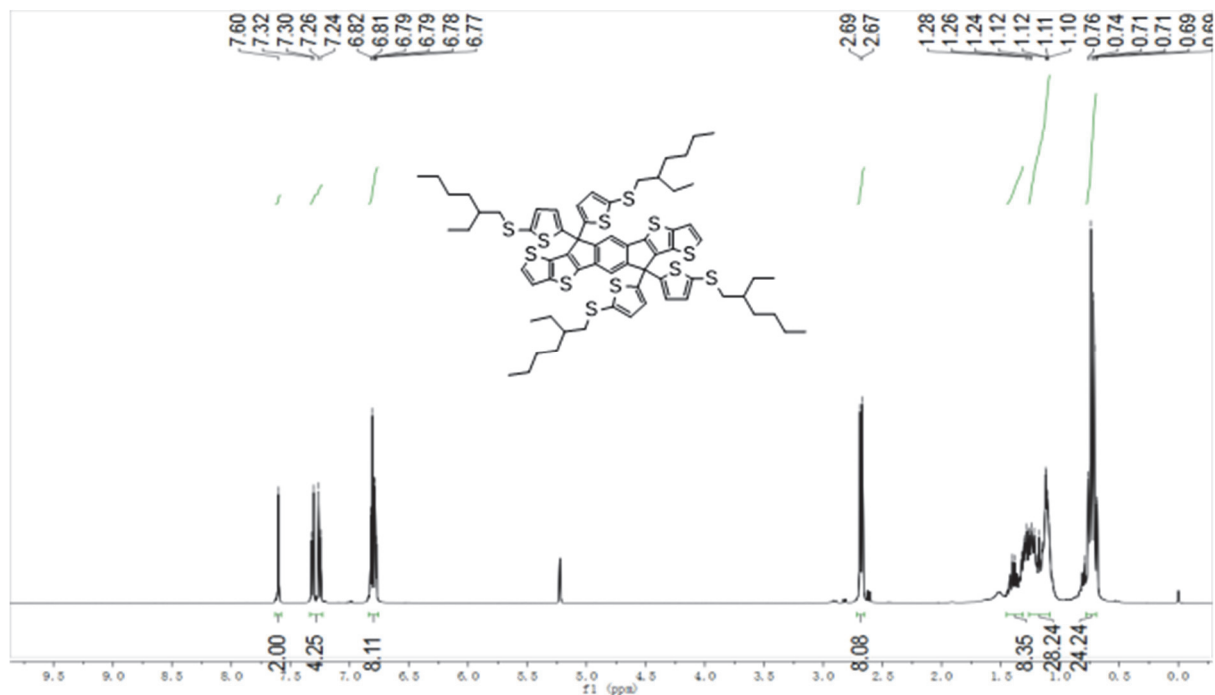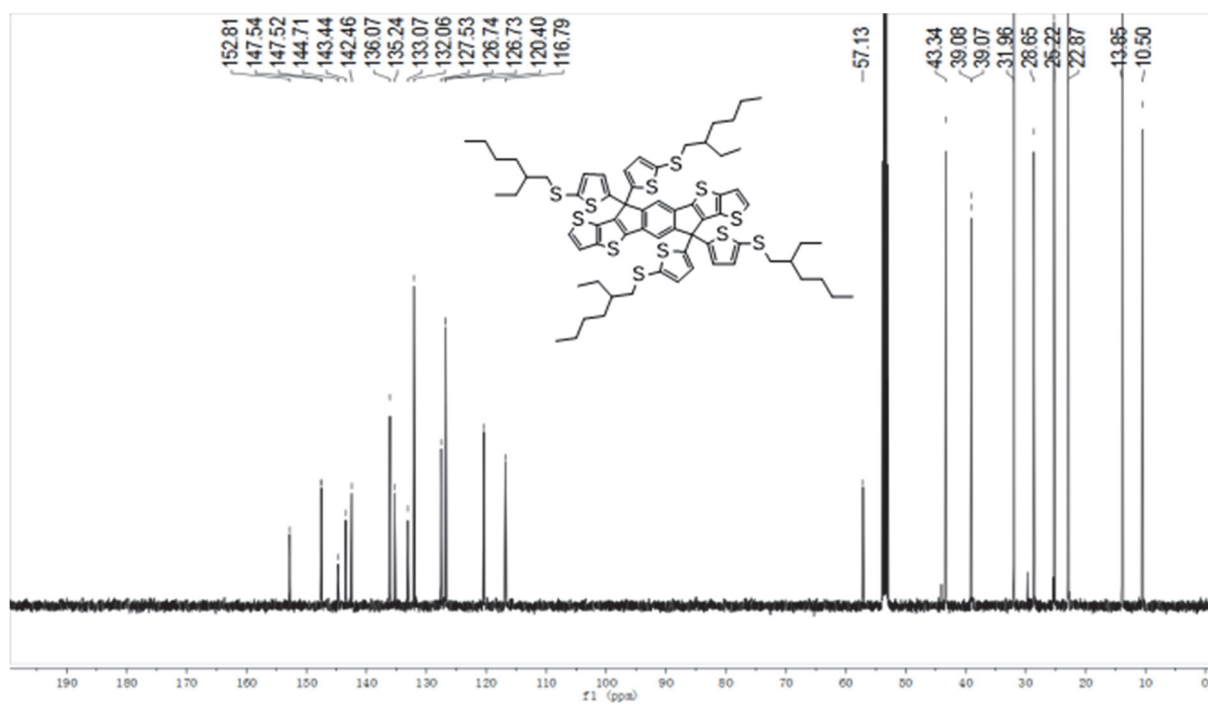
Figure S1. ^{1}H NMR data of ITIC-Th-s (2)

Figure S2. ^{13}C NMR data of ITIC-Th-s (2)
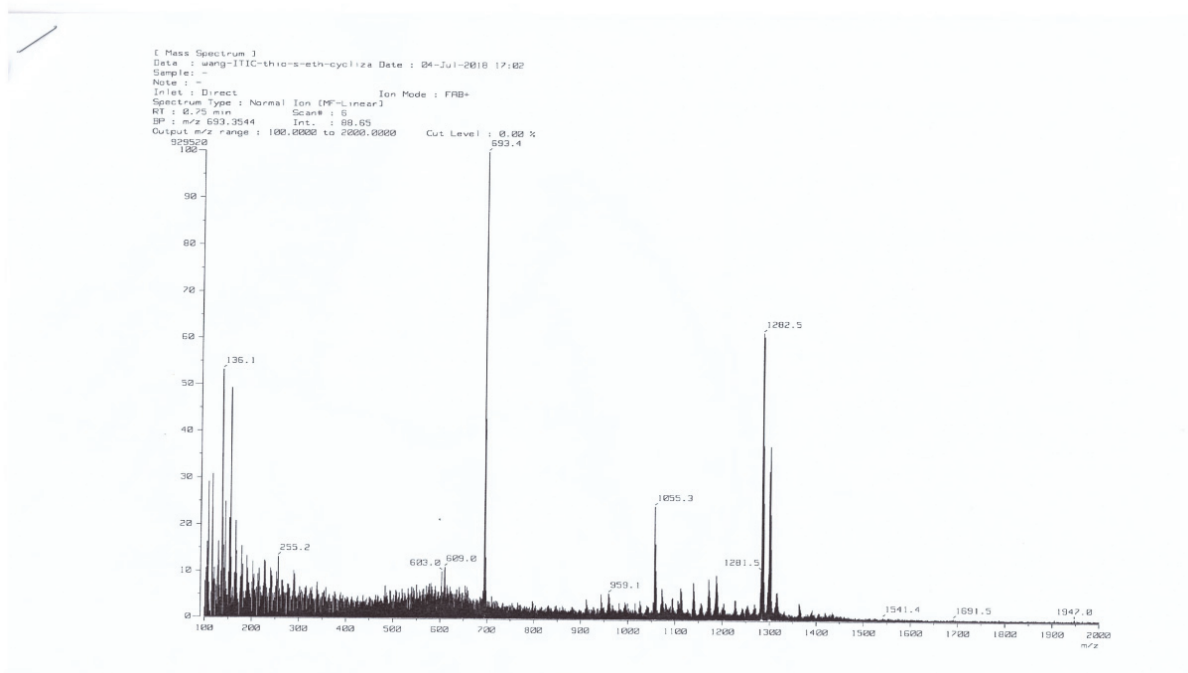
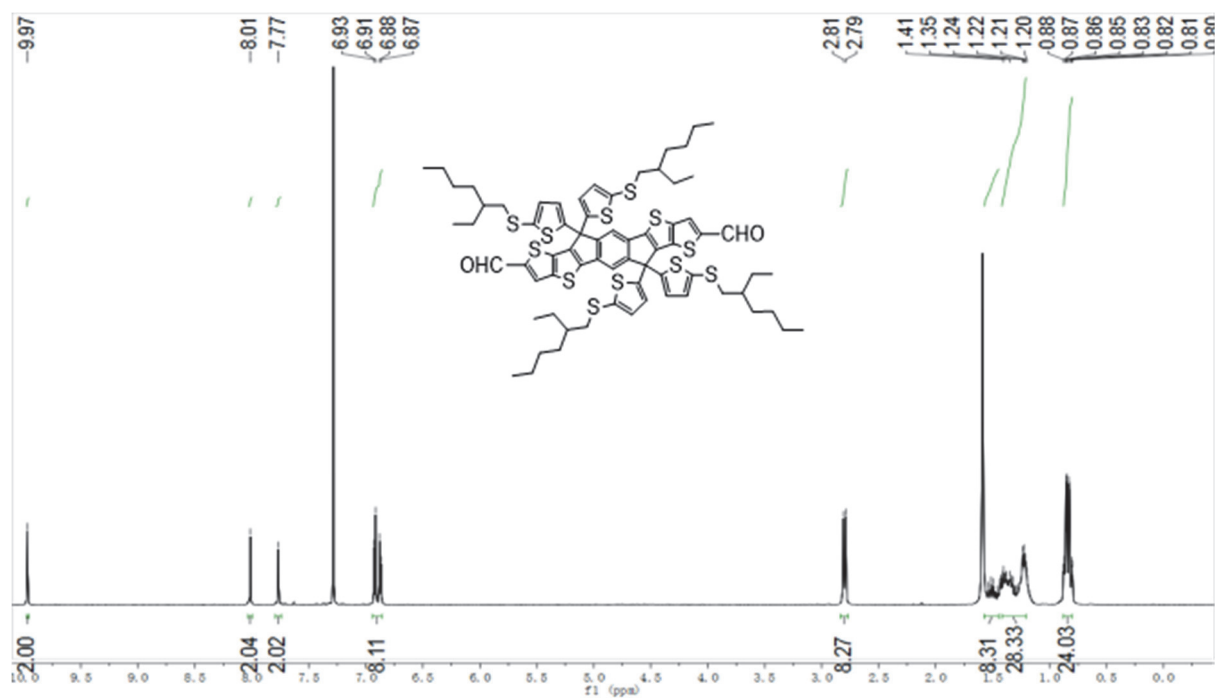**Figure S3**. FAB Mass data of ITIC-Th-s (2)

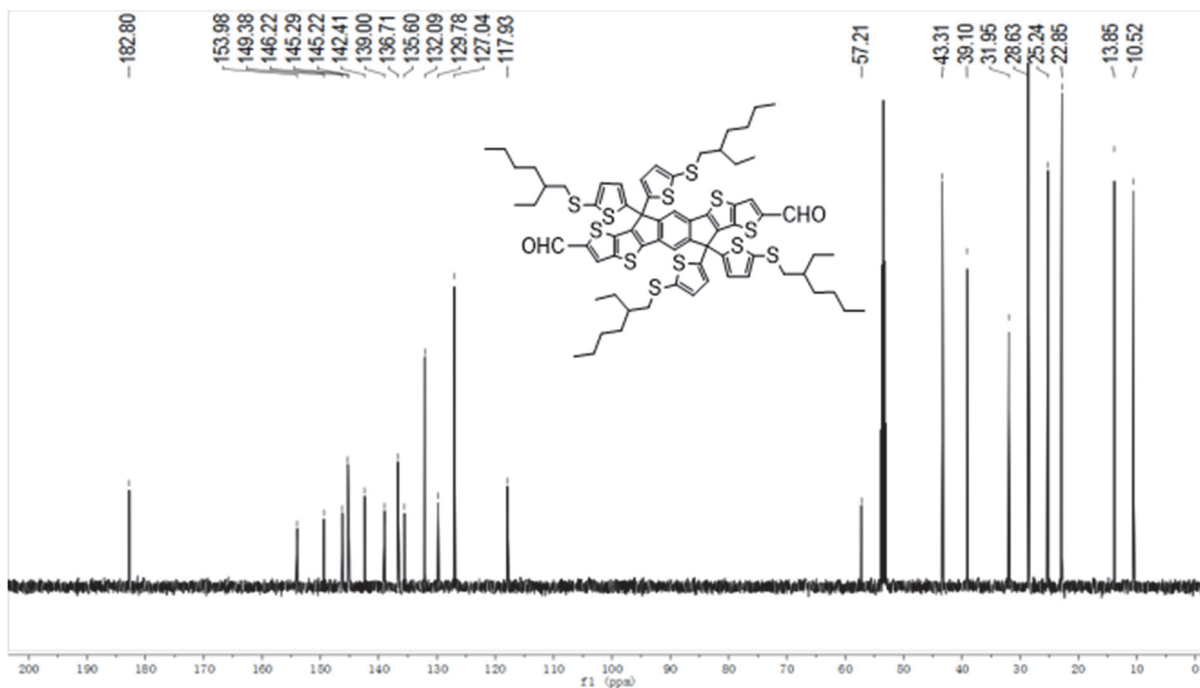**Figure S4**. ^{1}H NMR data of ITIC-Th-s-CHO

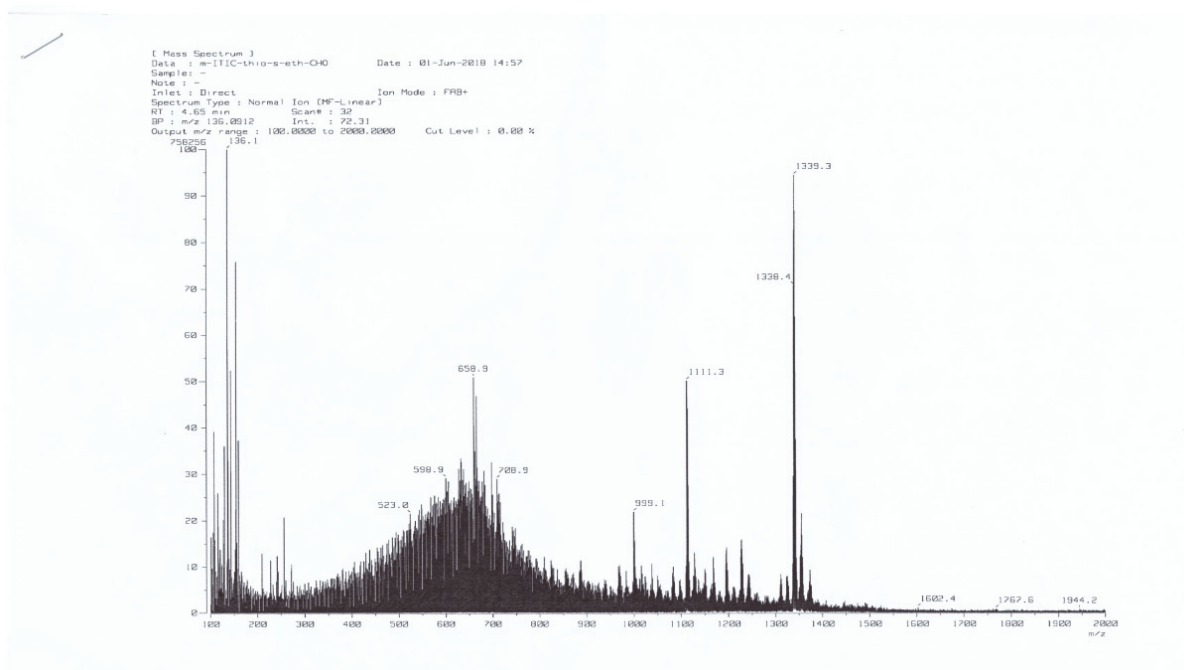**Figure S5**. ^{13}C NMR data of ITIC-Th-s-CHO

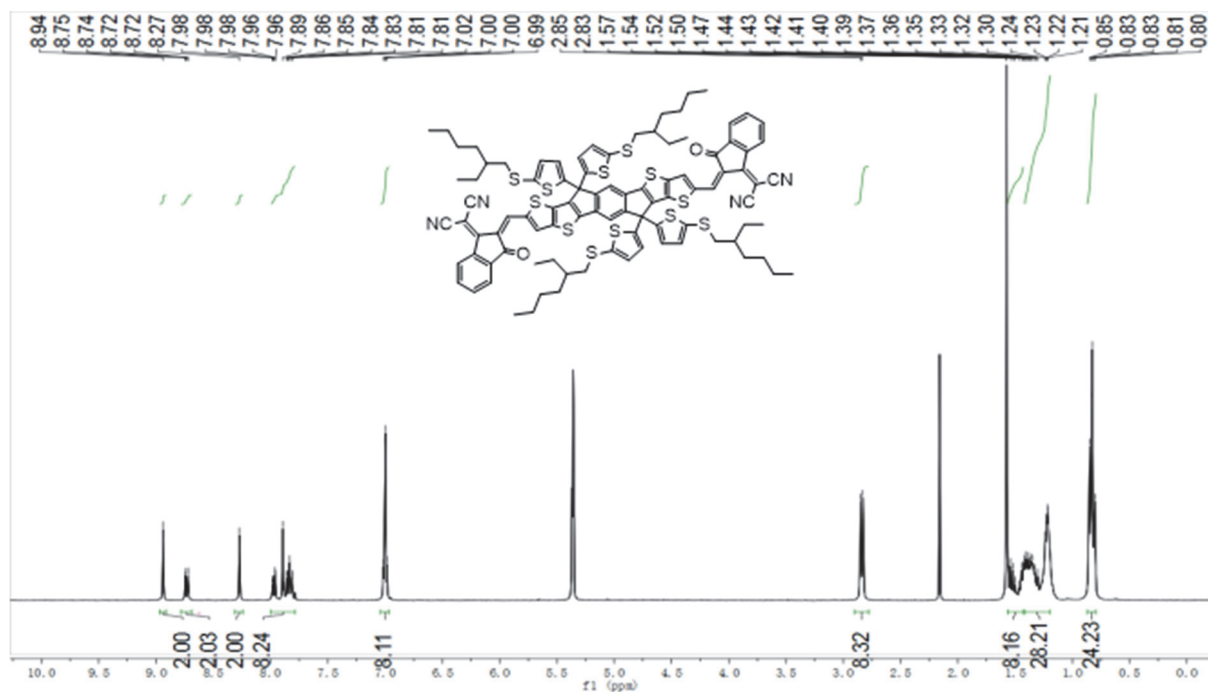**Figure S6**. FAB Mass data of ITIC-Th-s-CHO

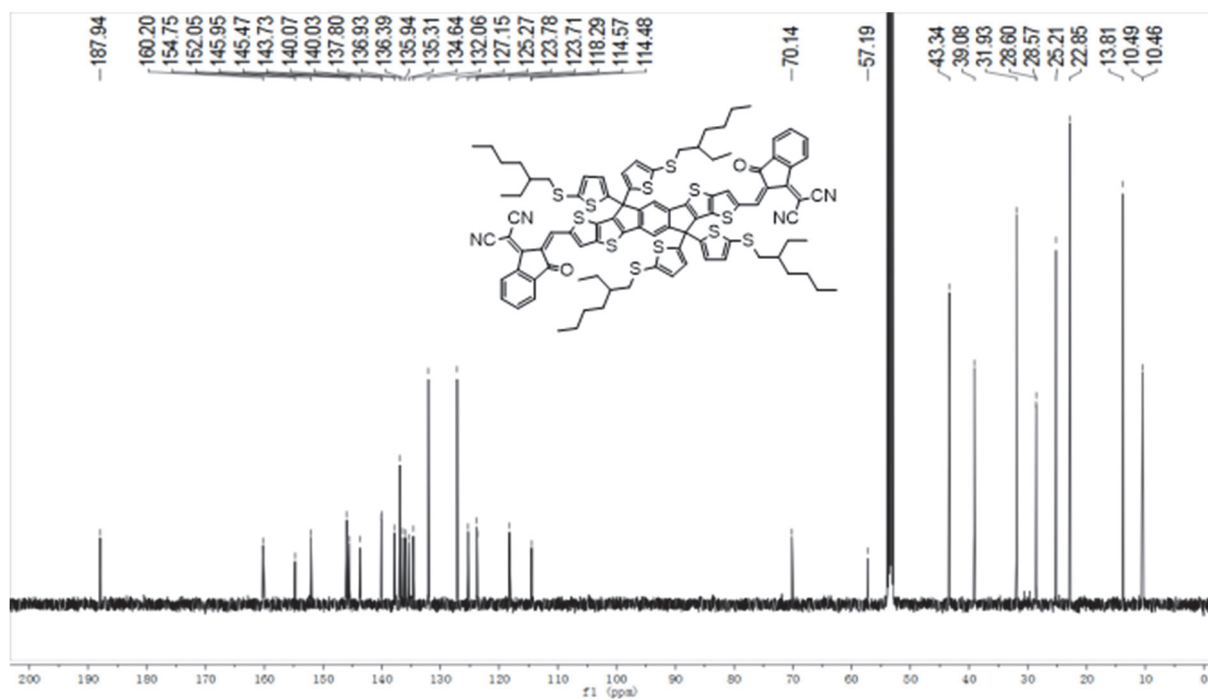**Figure S7**. ^{1}H NMR data of ITIC-Th-s

Figure S8. ^{13}C NMR data of ITIC-Th-s
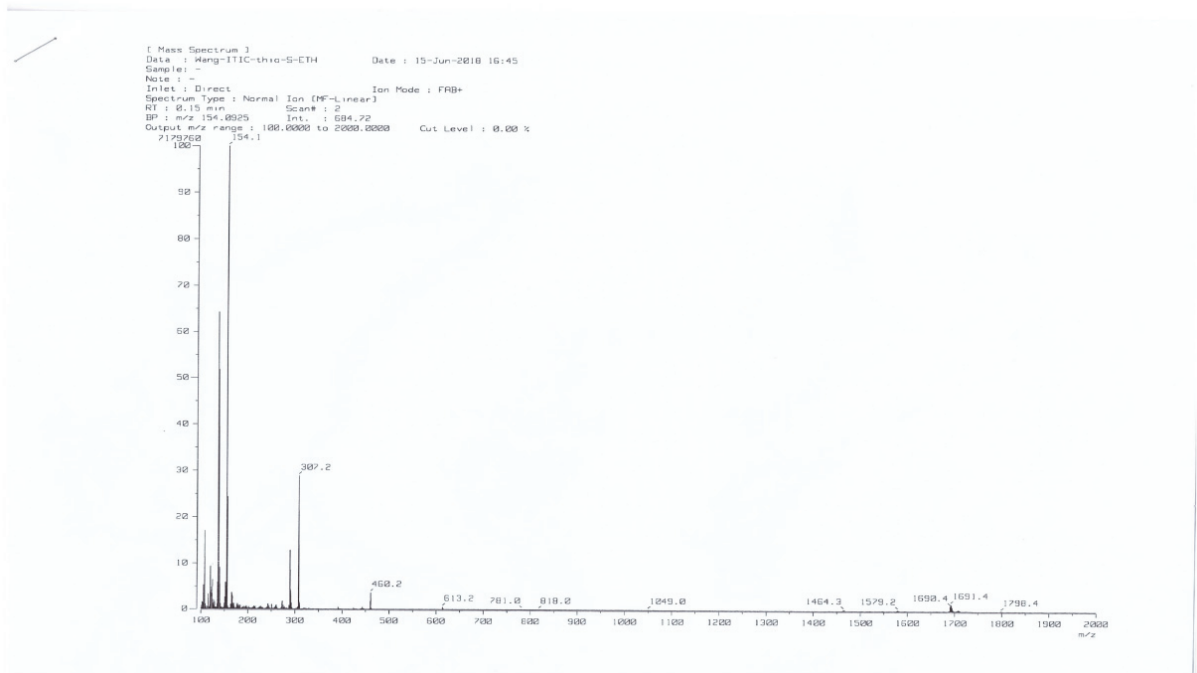
Figure S9. FAB Mass data of ITIC-Th-s
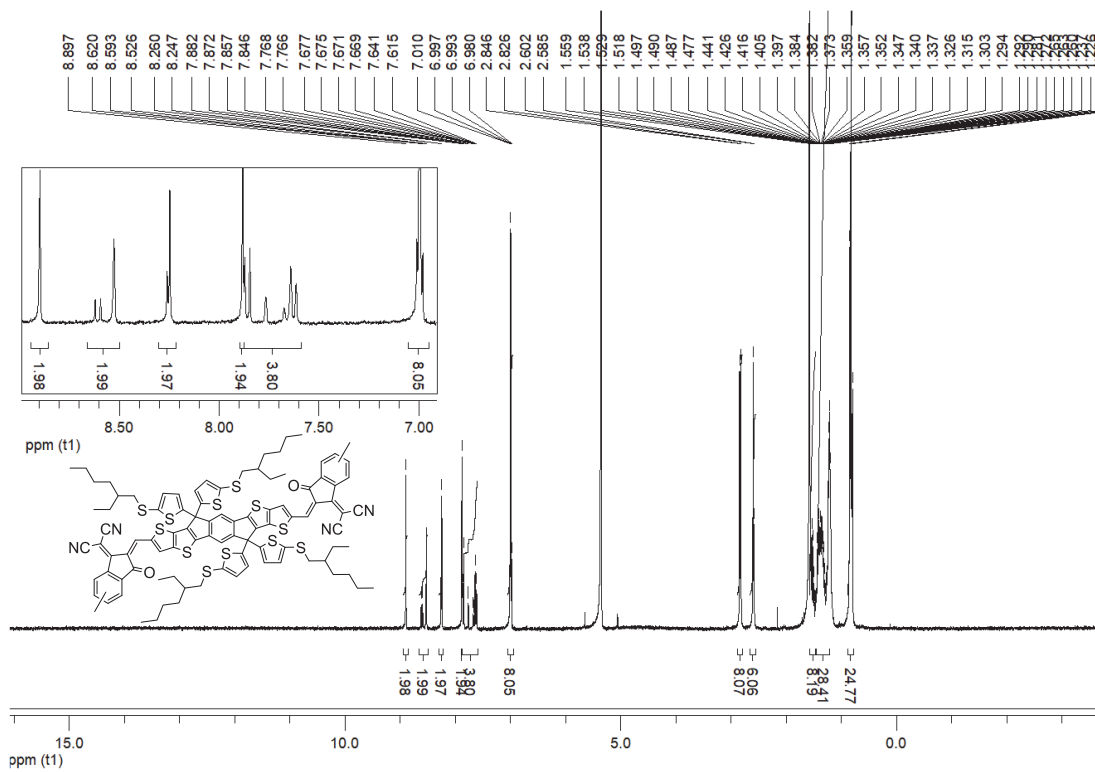
Figure S10. ^{1}H NMR data of ITIC-Th-s-me

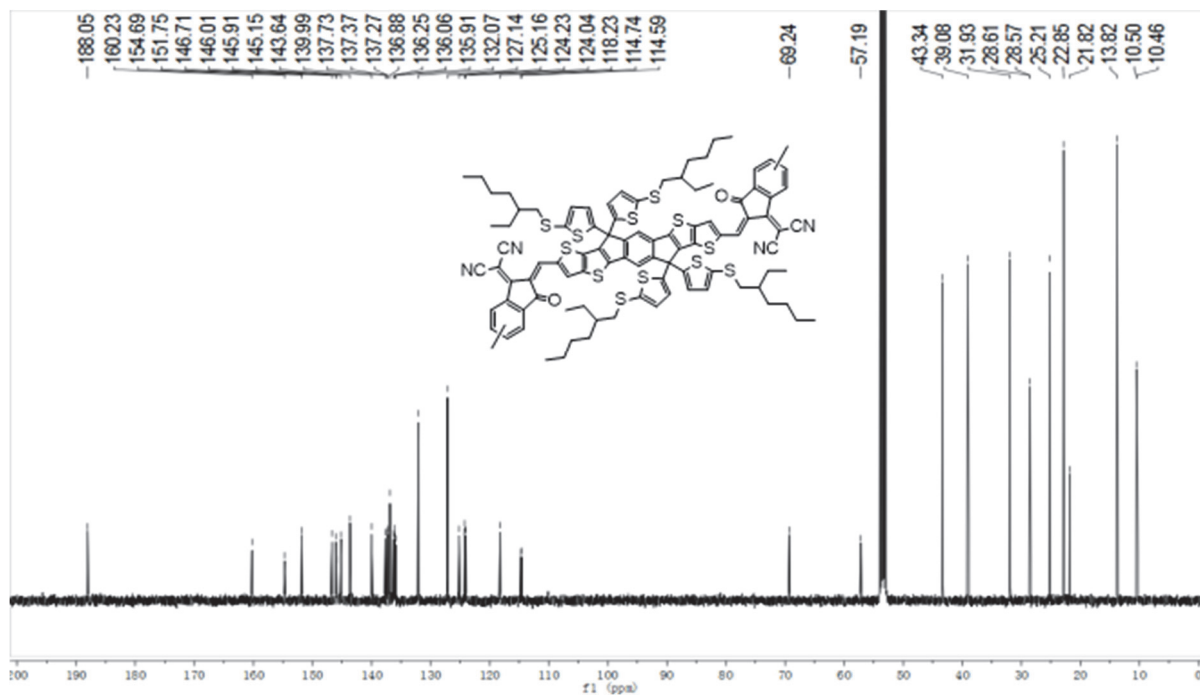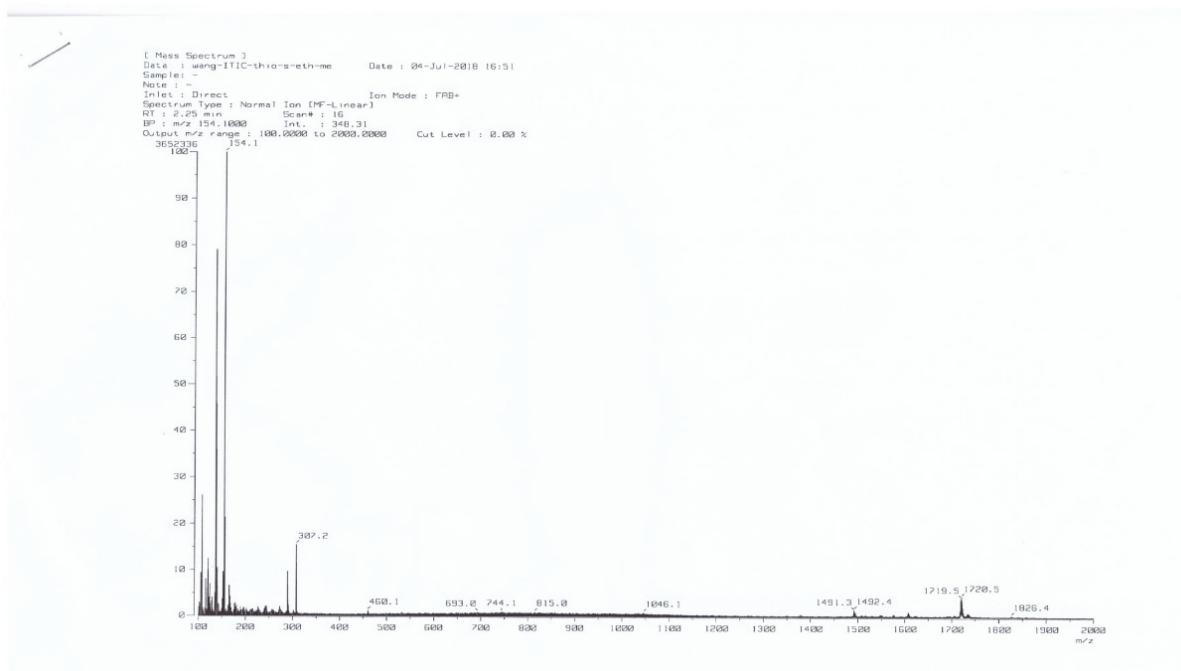**Figure S11**. ^{13}C NMR data of ITIC-Th-s-me

Figure S12. FAB Mass data of ITIC-Th-s-me

13
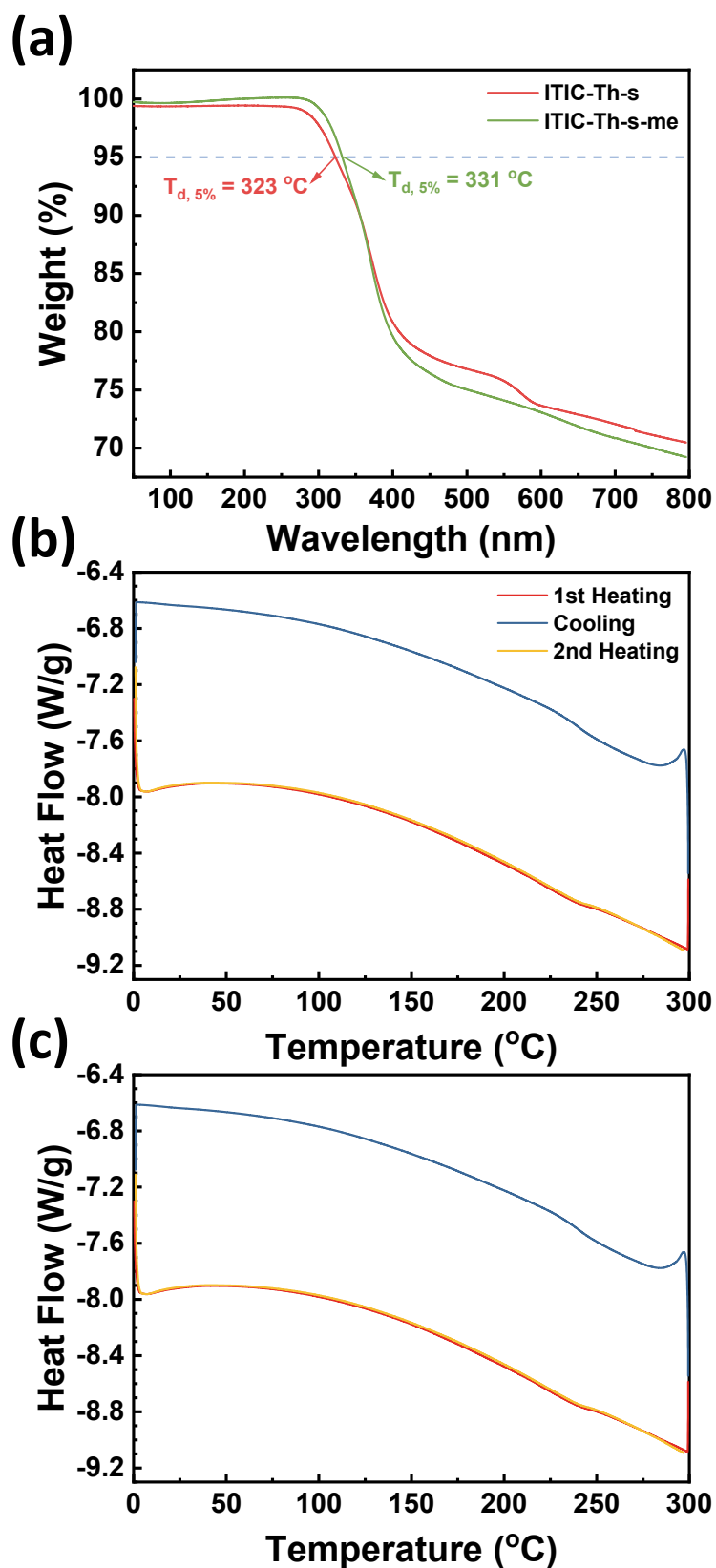
Figure S13. (a) Thermogravimetric analysis (TGA) and differential scanning calorimeter (DSC) of ITIC-Th-s and ITIC-Th-s-me. (b) Differential scanning calorimeter (DSC) of (b) ITIC-Th-s and (c) ITIC-Th-s-me.

14
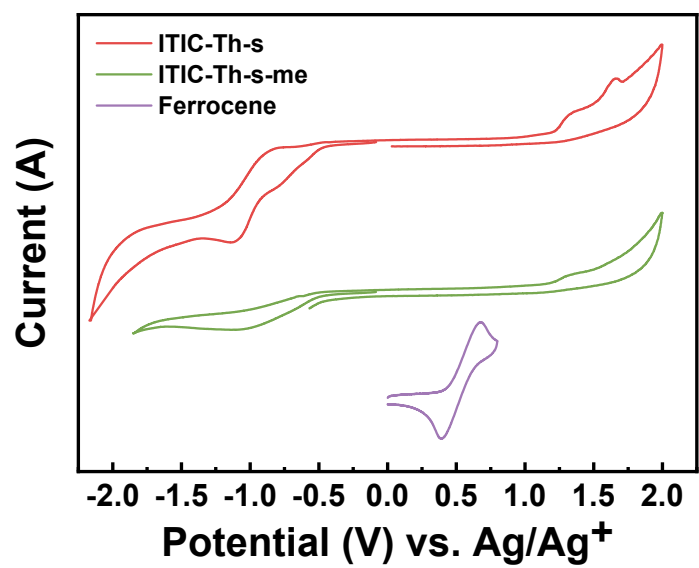
Figure S14. Cyclic voltammetry (CV) diagram of ITIC-Th-s and ITIC-Th-s-me.
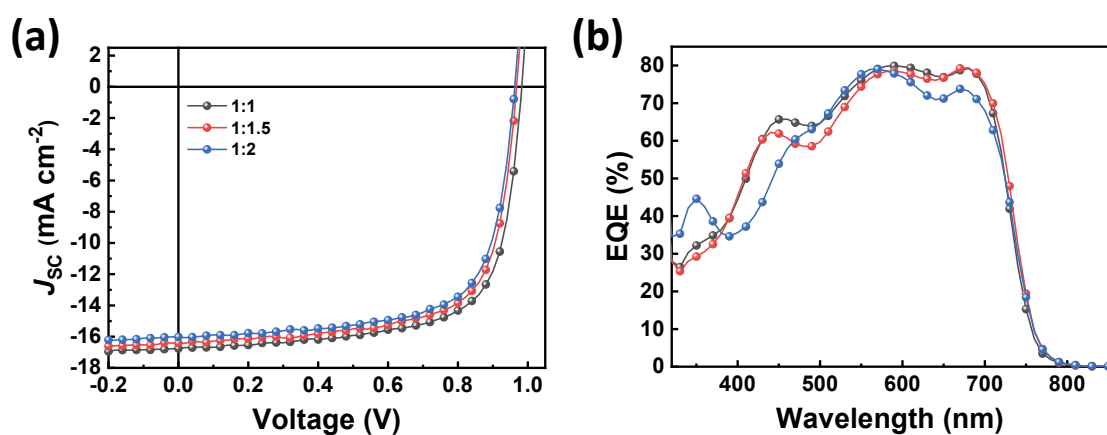
Figure S15. (a) *J–V* characteristics and (b) EQE spectrum of PM6:ITIC-Th-s-me based OPVs with various D:A ratios.

Table S1. Photovoltaic parameters of PM6:ITIC-Th-s-me based OPVs with various D:A ratios.

Active Layer	D:A Ratio (w/w)	J_{SC} (mA cm^{-2})	Cal. J_{SC} (mA cm^{-2})	V_{OC} (V)	FF	PCE (%)
PM6:ITIC-Th-s-me[a]	1:1	16.77	16.14	0.980	0.701	11.55
	1:1.5	16.38	15.96	0.974	0.694	11.08
	1:2	16.02	15.40	0.963	0.698	10.76

a) Under 0.5 vol% 1,8-diiodooctane (DIO) with thermal annealing at 100 ºC for 5 min.

Figure S16. (a) *J–V* characteristics and (b) EQE spectrum of PM6:ITIC-Th-s-me based OPVs with various additives in chlorobenzene (CB).

Table S2. Photovoltaic parameters of PM6:ITIC-Th-s-me based OPVs with various additives in CB.

Active Layer	Additive	J_{SC} (mA cm^{-2})	Cal. J_{SC} (mA cm^{-2})	V_{OC} (V)	FF	PCE (%)
PM6:ITIC-Th-s-me	w/o[a]	15.63	15.26	0.990	0.657	10.15
	DIO[b]	16.77	16.14	0.980	0.701	11.55
	DPE[b]	15.57	15.37	0.986	0.641	9.85
	CN[b]	15.06	14.87	0.999	0.650	9.77

a) Under thermal annealing at 100 ºC for 5 min.

b) Under 0.5 vol% DIO, diphenyl ether (DPE) and 1-chloronaphthalene (CN) with thermal annealing at 100 ºC for 5 min.
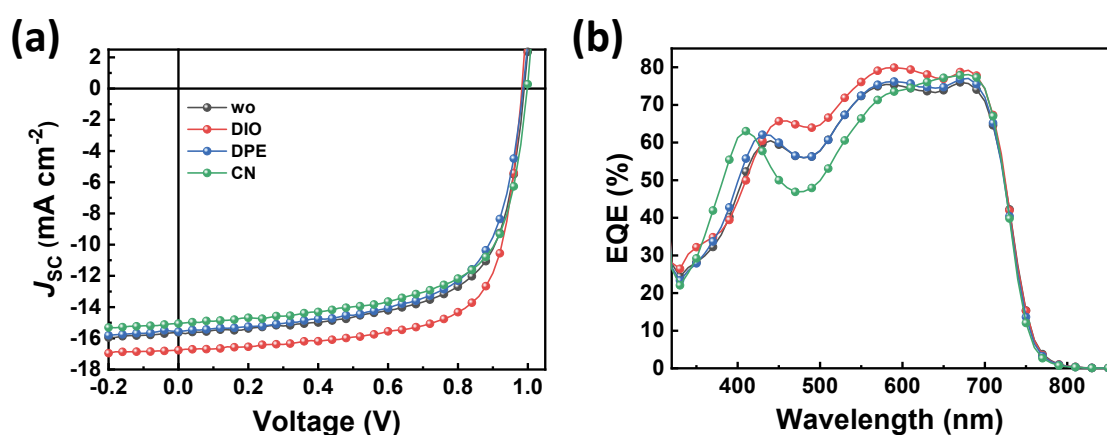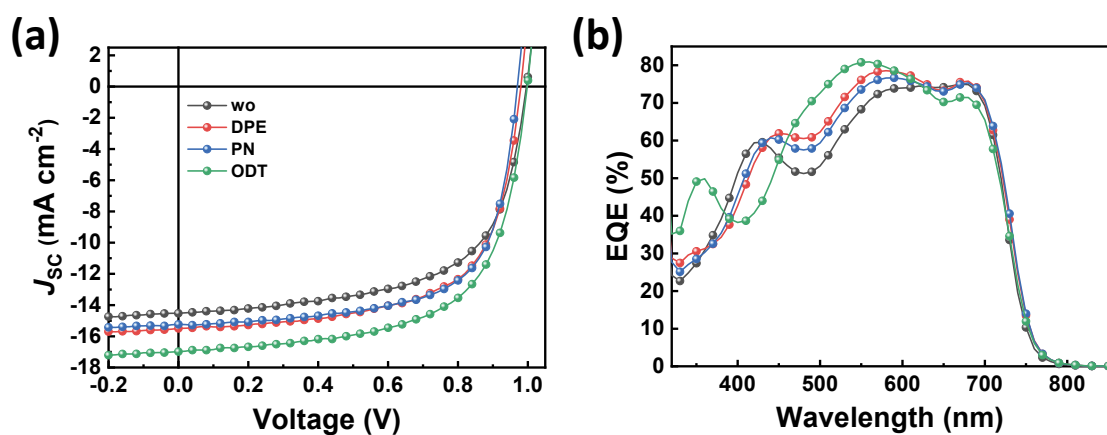
Figure S17. (a) *J–V* characteristics and (b) EQE spectrum of PM6:ITIC-Th-s-me based OPVs with various additives in xylene (Xyl).

Table S3. Photovoltaic parameters of PM6:ITIC-Th-s-me based OPVs with various additives in Xyl.

Active Layer	Additive	J_{SC} (mA cm^{-2})	Cal. J_{SC} (mA cm^{-2})	V_{OC} (V)	FF	PCE (%)
PM6:ITIC-Th-s-me	w/o[a]	14.53	14.66	0.996	0.623	9.02
	DPE[b]	15.64	15.54	0.979	0.645	9.88
	PN[b]	15.24	15.32	0.970	0.672	9.94
	ODT[b]	16.22	15.53	1.010	0.683	11.18

a) Under thermal annealing at 100 ºC for 5 min.

b) Under 0.5 vol% DPE, 1-phenylnaphthalene (PN) and 1, 8-octanedithiol (ODT) with thermal annealing at 100 ºC for 5 min.
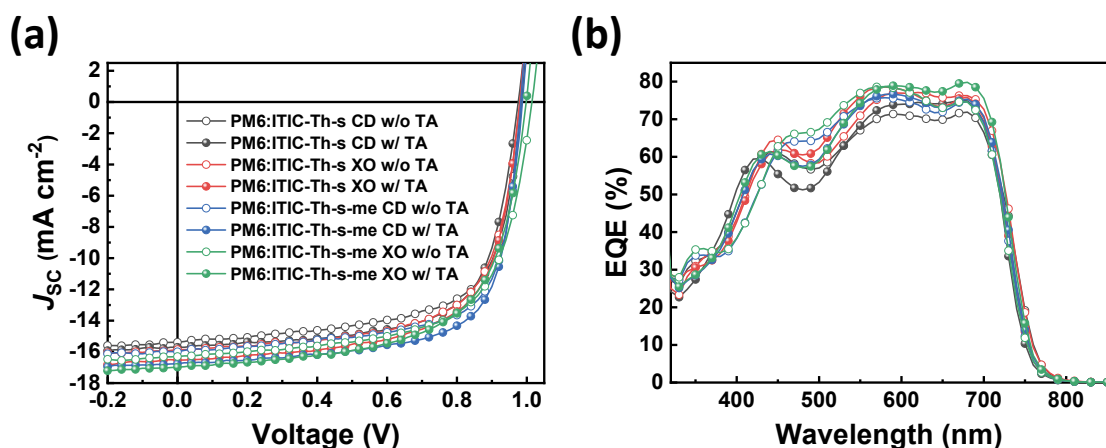
Figure S18. (a) *J–V* characteristics and (b) EQE spectrum of PM6:ITIC-Th-s and PM6:ITIC-Th-s-me based OPVs without and with thermal annealing treatments.

Table S4. Photovoltaic parameters of PM6:ITIC-Th-s and PM6:ITIC-Th-s-me based OPVs without and with thermal annealing treatments.

Active Layer	Solvents	TA (°C, min)	J_{SC} (mA cm^{-2})	Cal. J_{SC} (mA cm^{-2})	V_{OC} (V)	FF	PCE (%)
PM6:ITIC-Th-s	CD[a]	w/o	15.39	14.79	0.985	0.667	10.11
		(100, 5)	15.71	15.34	0.976	0.679	10.41
	XO[b]	w/o	15.86	15.64	0.981	0.669	10.40
		(100, 5)	16.53	15.75	0.980	0.663	10.74
PM6:ITIC-Th-s-me	CD[a]	w/o	15.99	15.24	0.988	0.696	10.99
		(100, 5)	16.77	16.14	0.983	0.701	11.55
	XO[b]	w/o	16.30	15.54	1.015	0.655	10.83
		(100, 5)	16.22	15.52	1.010	0.683	11.18

* Average values with standard deviations in the brackets are obtained from 10 devices.

a) Under CB:DIO (CD) (99.5:0.5, v/v)

b) Under Xyl:ODT (XO) (99.5:0.5, v/v).
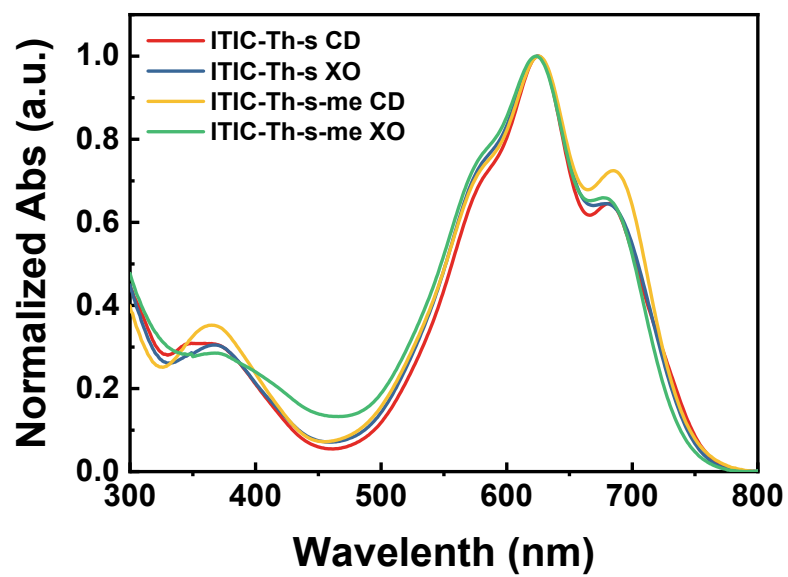
Figure S19. UV-vis spectrum of PM6:ITIC-Th-s and PM6:ITIC-Th-s-me blend film at the optimized condition.
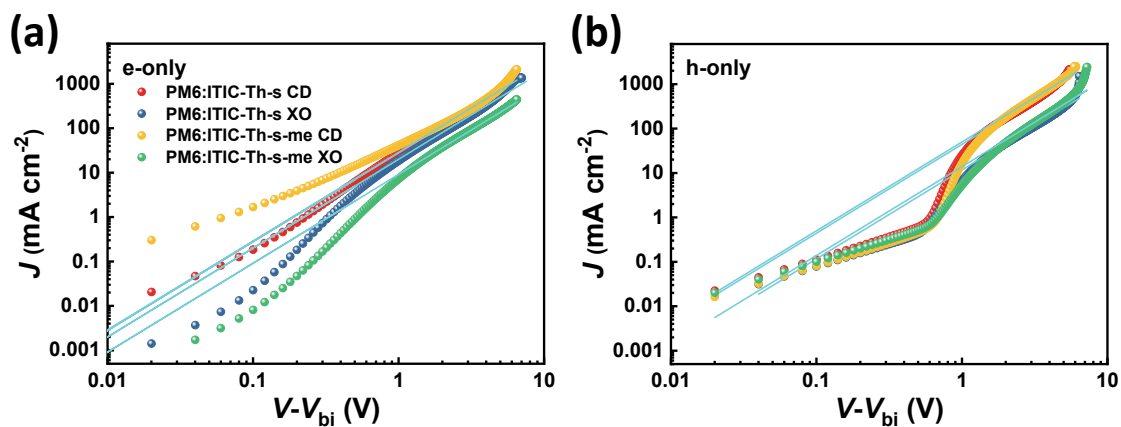
Figure S20. *J–V* characteristics of hole and electron only devices obtained by space charge limited current (SCLC) technique.

Table S5. Hole and electron mobilities of PM6:ITIC-Th-s and PM6:ITIC-Th-s-me blend films obtained by space charge limited current (SCLC) technique.

Active Layer	μ_e (cm^2 V^{-1} s^{-1})	μ_h (cm^2 V^{-1} s^{-1})	μ_e/μ_h	n_t (cm^{-3})
ITIC-Th-s CD	4.42×10^{-4}	1.75×10^{-4}	2.53	4.31×10^{16}
ITIC-Th-s XO	3.99×10^{-4}	1.48×10^{-4}	2.66	1.18×10^{16}
ITIC-Th-s-me CD	3.28×10^{-4}	1.50×10^{-4}	2.19	4.08×10^{16}
ITIC-Th-s-me XO	3.36×10^{-4}	1.42×10^{-4}	2.37	1.12×10^{16}
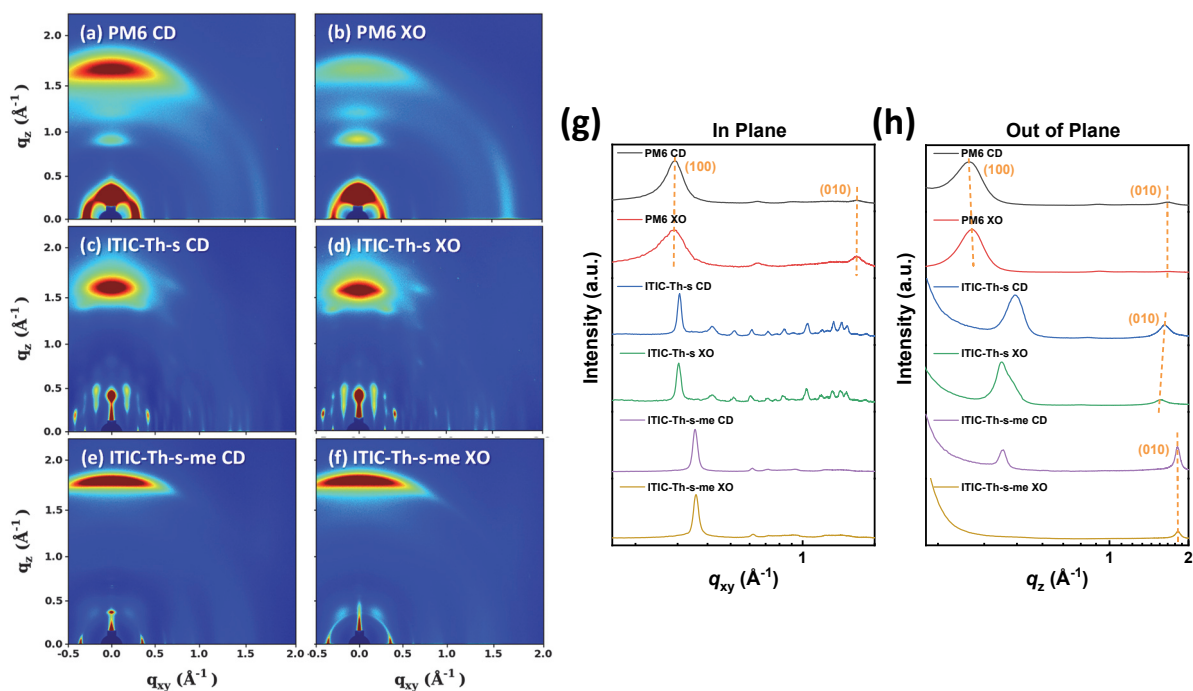
Figure S21. (a)–(f) 2D grazing incident wide angle X-ray scattering (GIWAXS) patterns and (g), (h) line-cut profiles of pristine PM6, ITIC-Th-s and ITIC-Th-s-me films.

Table S6. GIWAXS packing parameter of pristine PM6, ITIC-Th-s and ITIC-Th-s-me films.

Direction	Materials	(100)				(010)			
		q [$Å^{-1}$]	d_{100} [$Å$]	FWHM [$Å^{-1}$]	CCL_{100} [$Å$]	q [$Å^{-1}$]	d_{010} [$Å$]	FWHM [$Å^{-1}$]	CCL_{010} [$Å$]
IP	PM6 CD	0.29	21.50	0.028	34.53	-	-	-	-
OOP		0.29	21.52	0.043	22.33	1.65	3.81	0.099	9.67
IP	PM6 XO	0.30	20.88	0.034	28.38	-	-	-	-
OOP		0.29	21.50	0.038	25.35	1.69	3.72	0.087	10.96
IP	ITIC-Th-s CD	0.31	20.53	0.006	159.99	-	-	-	-
OOP		0.44	14.41	0.032	29.56	1.63	3.85	0.076	12.52
IP	ITIC-Th-s XO	0.30	20.71	0.007	141.60	-	-	-	-
OOP		0.39	16.17	0.033	29.11	1.57	4.02	0.080	11.97
IP	ITIC-Th-s-me CD	0.36	17.69	0.009	109.38	-	-	-	-
OOP		0.40	15.92	0.013	75.86	1.82	3.46	0.042	22.54
IP	ITIC-Th-s-me XO	0.36	17.50	0.009	100.83	-	-	-	-
OOP		-	-	-	-	1.82	3.45	0.046	20.73
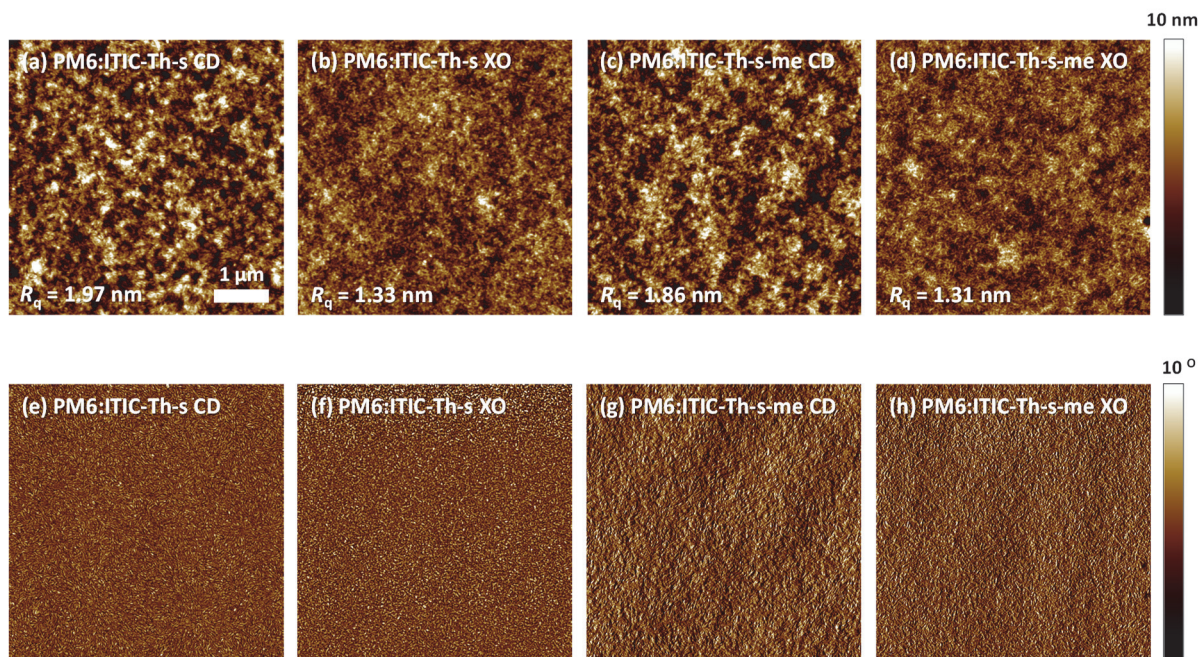
Figure S22. (a)–(d) Atomic force microscopy (AFM) height and (e)–(h) phase images of PM6:ITIC-Th-s and PM6:ITIC-Th-s-me blend films at the optimized condition. All the films were prepared on top of glass/ITO/PEDOT:PSS substrate.
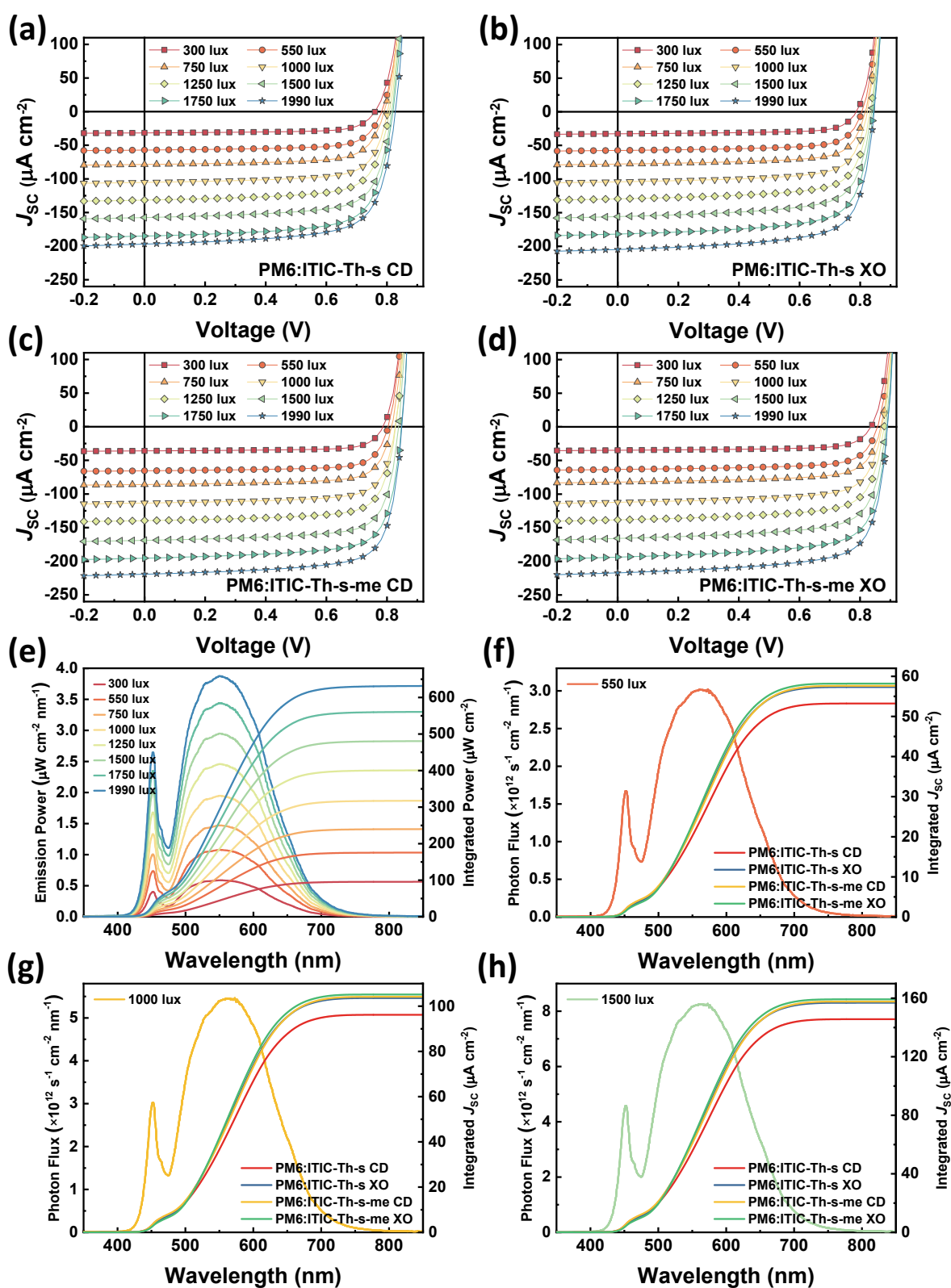
Figure S23. *J–V* characteristics of (a) PM6:ITIC-Th-s CD, (b) PM6:ITIC-Th-s XO, (c) PM6:ITIC-Th-s-me CD and (d) PM6:ITIC-Th-s-me XO based OPVs for a white LED light source at various light intensities. (e) Emission power spectra and integrated power of the light source at various light intensities. Photon flux spectrum of the LED light source and integrated current density of the OPVs under same condition at (f) 550, (g) 1000 and (h) 1500 lux.

Table S7. Photovoltaic parameters of PM6:ITIC-Th-s based OPVs for a white LED light source at various light intensities.

Active Layer	Light Intensity (lux)	P_{in} (μW cm^{-2})	J_{SC} (μA cm^{-2})	V_{OC} (V)	FF	P_{out} (μW cm^{-2})	PCE (%)
PM6:ITIC-Th-s CD	1990	633.2	200.9 (200.4±2.438)	0.830 (0.827±0.002)	0.728 (0.724±0.006)	121.4 (119.9±0.893)	19.17 (18.93±0.141)
	1750	562.1	185.1 (181.8±2.133)	0.820 (0.822±0.002)	0.716 (0.715±0.002)	108.7 (106.8±1.148)	19.51 (19.17±0.206)
	1500	481.9	157.5 (154.7±1.448)	0.816 (0.818±0.003)	0.726 (0.726±0.002)	93.23 (91.90±0.645)	19.53 (19.25±0.135)
	1250	401.8	131.5 (128.6±2.174)	0.808 (0.810±0.002)	0.721 (0.718±0.003)	76.60 (74.75±1.101)	19.26 (18.79±0.277)
	1000	318.3	105.2 (103.5±1.328)	0.802 (0.803±0.002)	0.728 (0.728±0.001)	61.41 (60.56±0.643)	19.30 (19.03±0.202)
	750	240.4	78.56 (76.35±1.298)	0.791 (0.792±0.002)	0.722 (0.720±0.003)	44.82 (43.51±0.630)	18.78 (18.23±0.264)
	550	176.1	57.16 (56.31±0.439)	0.783 (0.781±0.002)	0.721 (0.719±0.003)	32.27 (31.63±0.309)	18.43 (18.07±0.176)
	300	96.05	31.60 (31.26±0.215)	0.761 (0.761±0.002)	0.719 (0.719±0.003)	17.29 (17.09±0.109)	18.11 (17.90±0.114)
PM6:ITIC-Th-s XO	1990	633.2	204.8 (203.2±3.019)	0.846 (0.843±0.004)	0.717 (0.716±0.003)	124.2 (122.5±1.624)	19.61 (19.34±0.256)
	1750	562.1	181.8 (179.0±3.249)	0.843 (0.840±0.004)	0.716 (0.713±0.003)	109.7 (107.2±1.660)	19.70 (19.24±0.298)
	1500	481.9	155.9 (153.3±2.635)	0.838 (0.835±0.004)	0.714 (0.716±0.003)	93.28 (91.61±1.186)	19.54 (19.19±0.248)
	1250	401.8	129.5 (125.9±2.411)	0.832 (0.830±0.003)	0.718 (0.717±0.002)	77.41 (74.96±1.548)	19.46 (18.84±0.389)
	1000	318.3	104.1 (100.7±2.167)	0.823 (0.823±0.003)	0.720 (0.719±0.004)	61.69 (59.57±1.187)	19.38 (18.72±0.373)
	750	240.4	77.73 (76.71±1.246)	0.817 (0.813±0.003)	0.719 (0.717±0.003)	45.63 (44.71±0.614)	19.11 (18.73±0.257)
	550	176.1	57.49 (56.93±0.599)	0.805 (0.805±0.001)	0.717 (0.718±0.006)	33.20 (32.88±0.324)	18.97 (18.78±0.185)
	300	96.05	32.72 (31.84±0.636)	0.786 (0.783±0.003)	0.715 (0.714±0.004)	18.39 (17.79±0.332)	19.26 (18.63±0.348)

* Average values with standard deviations in the brackets are obtained from 10 devices.

Table S8. Photovoltaic parameters of PM6:ITIC-Th-s-me based OPVs for a white LED light source at various light intensities.

Active Layer	Light Intensity (lux)	P_{in} (μW cm^{-2})	J_{SC} (μA cm^{-2})	V_{OC} (V)	FF	P_{out} (μW cm^{-2})	PCE (%)
PM6:ITIC-Th-s-me CD	1990	633.2	219.3 (214.1±3.301)	0.849 (0.844±0.003)	0.749 (0.746±0.005)	139.4 (134.9±2.445)	22.02 (21.30±0.386)
	1750	562.1	195.5 (192.9±1.903)	0.847 (0.844±0.003)	0.749 (0.749±0.004)	124.1 (121.9±1.244)	22.28 (21.89±0.223)
	1500	481.9	169.0 (165.8±1.911)	0.838 (0.836±0.004)	0.756 (0.749±0.004)	107.1 (103.9±1.178)	22.43 (21.76±0.247)
	1250	401.8	139.6 (137.5±1.439)	0.828 (0.831±0.003)	0.752 (0.749±0.005)	86.93 (85.51±0.906)	21.85 (21.49±0.228)
	1000	318.3	113.5 (110.7±1.614)	0.827 (0.826±0.005)	0.748 (0.747±0.004)	70.19 (68.39±0.815)	22.05 (21.49±0.256)
	750	240.4	85.89 (84.56±0.764)	0.815 (0.815±0.002)	0.749 (0.750±0.003)	52.45 (51.65±0.417)	21.97 (21.64±0.174)
	550	176.1	65.52 (63.78±0.959)	0.803 (0.806±0.003)	0.750 (0.746±0.003)	39.45 (38.34±0.598)	22.54 (21.90±0.342)
	300	96.05	35.93 (35.68±0.190)	0.786 (0.784±0.005)	0.746 (0.735±0.006)	21.06 (20.57±0.215)	22.06 (21.55±0.225)
PM6:ITIC-Th-s-me XO	1990	633.2	217.2 (215.4±1.001)	0.890 (0.891±0.003)	0.731 (0.730±0.003)	141.3 (140.0±0.625)	22.30 (22.10±0.099)
	1750	562.1	193.7 (192.2±1.480)	0.889 (0.888±0.002)	0.729 (0.724±0.005)	125.5 (123.6±1.436)	22.54 (22.19±0.258)
	1500	481.9	165.9 (164.2±1.695)	0.885 (0.882±0.002)	0.726 (0.723±0.004)	106.6 (104.7±1.044)	22.33 (21.92±0.219)
	1250	401.8	138.3 (136.9±1.139)	0.880 (0.877±0.003)	0.722 (0.720±0.003)	87.81 (86.39±0.737)	22.07 (21.72±0.185)
	1000	318.3	112.2 (110.4±1.398)	0.872 (0.870±0.004)	0.720 (0.723±0.003)	70.49 (69.43±0.772)	22.15 (21.81±0.243)
	750	240.4	82.13 (81.10±0.610)	0.868 (0.864±0.002)	0.720 (0.716±0.005)	51.35 (50.18±0.483)	21.51 (21.02±0.610)
	550	176.1	63.36 (61.87±1.018)	0.857 (0.855±0.002)	0.721 (0.720±0.003)	39.17 (38.09±0.606)	22.38 (21.76±0.346)
	300	96.05	34.80 (34.39±0.331)	0.836 (0.835±0.003)	0.721 (0.715±0.004)	20.97 (20.54±0.262)	21.96 (21.51±0.274)

* Average values with standard deviations in the brackets are obtained from 10 devices.
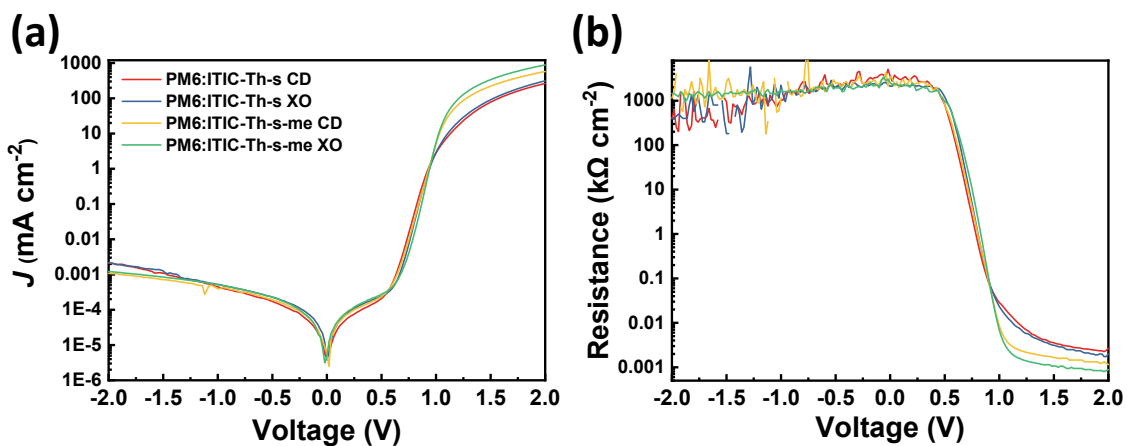
Figure S24. (a) *J–V* characteristics of PM6:ITIC-Th-s and PM6:ITIC-Th-s-me based OPVs in the dark condition and (b) the differential resistance derived from (a).
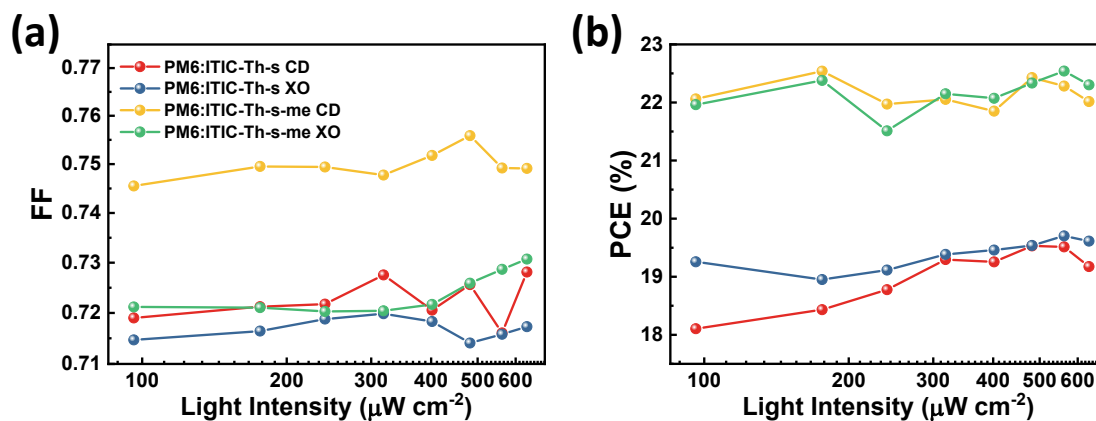

Figure S25. (a) Fill factor (FF) and (b) power conversion efficiency (PCE) dependence on incident light intensity for PM6:ITIC-Th-s and PM6:ITIC-Th-s-me based OPVs.

Table S9. Summary of photovoltaic parameters of the IOPVs processed from non-halogenated solvent mixture or host solvents in recently reported literature.

Active layer	Host Solvent	Solvent Additive	Light Source (Intensity)	J_{SC} (µA cm^{-2})	V_{OC} (V)	FF	P_{out} (µW cm^{-2})	PCE (%)
PPDT2FBT:ITIC-F[3]	o-xylene	DPE	LED (10000 lux)	817	0.67	0.56	303	9.80
PTQ10:tPDI$_2$N-EH[4]	Toluene	DPE	LED (2000 lux)	139	1.07	0.48	71.4	11.7
FBT:PC$_{61}$BM:PDI[5]	o-xylene	*p*-anisaldehyde	LED (2000 lux)	167	0.72	0.73	88.0	15.5
PJ50:IT-4F[6]	Toluene	-	LED (500 lux)	54.8	0.69	0.73	27.9	17.4
PTB7-Th:PC$_{71}$BM[7]	o-xylene	-	LED (~3000 lux)	1022	0.74	0.62	469	14.3
PV-X plus[8]	o-xylene	-	LED (500 lux)	53.3	0.67	0.77	-	19.3
J52-Cl:BTA3:BTA1[9]	Tetrahydrofuran	-	LED (1000 lux)	96.7	1.12	0.80	86.9	28.8
PM6:ITIC-Th-s-me*	o-xylene	ODT	LED (500 lux)	39.1	0.86	0.72	39.2	22.4

* The photovoltaic parameters of the IOPVs in our work were also indicated for comparison.

References

1. W. Gao, Q. An, R. Ming, D. Xie, K. Wu, Z. Luo, Y. Zou, F. Zhang and C. Yang, *Adv. Funct. Mater.*, 2017, **27**, 1702194.

2. P. N. Murgatroyd, *J. Phys. D: Appl. Phys.*, 1970, **3**, 151–156.

3. S. V. Dayneko, M. Pahlevani and G. C. Welch, *ACS Appl. Mater. Interfaces*, 2019, **11**, 46017–46025.

4. F. Tintori, A. Laventure, J. D. B. Koenig and G. C. Welch, *J. Mater. Chem. C*, 2020, **8**, 13430–13438.

5. M. E. Farahat, A. Laventure, M. A. Anderson, M. Mainville, F. Tintori, M. Leclerc, E. L. Ratcliff and G. C. Welch, *ACS Appl. Mater. Interfaces*, 2020, **12**, 43684–43693.

6. S. H. Park, N. Y. Kwon, H. J. Kim, E. Cho, H. Kang, A. K. Harit, H. Y. Woo, H. J. Yoon, M. J. Cho and D. H. Choi, *ACS Appl. Mater. Interfaces*, 2021, **13**, 13487–13498.

7. M. Cui, A. Lv and Z. Ma, *ChemPhysChem*, 2022, **23**, e202200091.

8. D. Müller, L. Campos Guzmán, E. Jiang, B. Zimmermann and U. Würfel, *Sol. RRL*, 2022, **6**, 2200175.

9. Q. Wu, Y. Yu, X. Xia, Y. Gao, T. Wang, R. Sun, J. Guo, S. Wang, G. Xie, X. Lu, E. Zhou and J. Min, *Joule*, 2022, **6**, 2138–2151.